Extremely strong room-temperature transient photocurrent-detected magnetic resonance in organic devices

Ying Chen,[1,*] Rui Liu,[1] Min Cai,[1] Ruth Shinar,[2] and Joseph Shinar[1,*]

[1]*Ames Laboratory—USDOE and Physics and Astronomy Department, Iowa State University, Ames, Iowa 50011, USA*

[2]*Microelectronics Research Center and Electrical and Computer Engineering Department, Iowa State University, Ames, Iowa 50011, USA*

(Received 19 April 2012; revised manuscript received 26 November 2012; published 26 December 2012)

An extremely strong room-temperature photocurrent- (PC- or I_{PC}-) detected magnetic resonance (PCDMR) that elucidates transport and trapping phenomena in organic devices, in particular solar cells, is described. When monitoring the transient PCDMR in indium tin oxide (ITO)/poly(2-methoxy-5-(2′-ethyl)-hexoxy-1,4-phenylenevinylene) (MEH-PPV)/Al devices, where the MEH-PPV film was baked overnight at 100 °C in O_2, it is observed that $|\Delta I_{PC}/I_{PC}|$ peaks at values $\gg 1$, where ΔI_{PC} is the change in I_{PC} induced by magnetic resonance conditions. Importantly, ΔI_{PC} and I_{PC} are of different origin. The mechanism most likely responsible for this effect is the spin-dependent formation of spinless bipolarons adjacent to negatively charged deep traps, apparently induced in particular by oxygen centers, to form trions.

DOI: 10.1103/PhysRevB.86.235442 PACS number(s): 76.70.Hb, 73.50.Pz, 81.05.Fb, 82.35.Cd

I. INTRODUCTION

Magnetic field effects (MFEs) and optically and electrically detected magnetic resonance (ODMR and EDMR) have been among the most powerful techniques for elucidating the nature and dynamics of excitons, polarons, and bipolarons in π-conjugated materials and devices.[1–7] They probe these materials and devices by studying changes in an optical or electrical quantity induced by magnetic resonance conditions. Typically, these conditions are satisfied by applying an appropriate microwave field at the dc magnetic field for resonance. To enhance the signal-to-noise ratio of the monitored quantity, the microwave field is modulated (chopped) at some reference frequency f_μ, and the signal is monitored by a lock-in amplifier.

Recently, MFE, ODMR, and EDMR studies have gained additional attention due to their potential to spawn an organic spintronic technology revolution.[8–15] Yet, these studies have fallen short in identifying major trapping sites and clarifying their role in these materials and devices. Additionally, all organic MFEs, ODMRs, and EDMRs reported to date are either small (the magnetic field- or resonance-induced relative change in the measured quantity $|\Delta I/I| \leqslant 0.03$) or significant only at low temperatures.[13] This begs the question whether stronger responses may be obtained.

This paper addresses both foregoing issues by describing the room-temperature photocurrent- (PC- or I_{PC}-) detected magnetic resonance (PCDMR) in single-layer indium tin oxide (ITO)/poly(2-methoxy-5-(2′-ethyl)-hexoxy-1,4-phenylenevinylene (MEH-PPV)/Al devices, where 9.35-GHz X-band magnetic resonance conditions induce an extremely strong transient $\Delta I_{PC}/I_{PC}$ when the MEH-PPV film is baked overnight at 100 °C in pure O_2. Interestingly, ΔI_{PC} is relatively independent of I_{PC}. By comparing these devices with those containing unbaked MEH-PPV (kept in vacuum), we conclude that the mechanism most likely responsible for this strong effect is the strongly spin-dependent formation of spinless positive bipolarons bp^{++} adjacent to negatively charged deep traps, apparently induced by oxygen, to form trions.

II. EXPERIMENTAL

For sample preparation, Sigma-Aldrich MEH-PPV ($40\,000 \leqslant M_n \leqslant 70\,000$) was dissolved in chlorobenzene and spin-coated on a Colorado Concept Coatings ~140-nm-thick 10-Ω/sq ITO-coated glass at 2000 rpm. It was then baked at 60 °C for 30 min in an argon-filled glove box. The Al was thermally evaporated on the MEH-PPV in a vacuum chamber (background $\sim 10^{-6}$ mbar) inside the glove box.

The samples were placed in the quartz "finger" dewar of an Oxford Instruments cryostat inside an optically accessible 9.35-GHz X-band microwave cavity.[1–3,5–7] I_{PC} was excited at 488 nm by a Spectra-Physics Ar^+ laser. ΔI_{PC} was detected by monitoring the voltage across a standard resistor in series with the sample. For time-resolved measurements, that voltage was monitored directly by a digital storage oscilloscope. For cw measurements it was monitored by a lock-in amplifier at f_μ. Since the PCDMR is sensitive to uncontrolled fabrication variables, all comparisons were made to a reference cell from the same batch.

Secondary ion mass spectrometry (SIMS) depth profiles using a 4-kV Cs^+ beam were provided by Evans Analytical Group using a PHI 6300 system.

III. EXTREMELY STRONG PCDMR AND ITS ORIGIN

Figure 1(a) shows our central result. It compares the time-resolved room-temperature I_{PC} vs time t on resonance at $H_{ON} = 3330.2$ G and off-resonance at $H_{OFF} = 3283.0$ G of an ITO/MEH-PPV/Al sample, with the MEH-PPV film baked overnight in O_2. Baking in O_2 greatly strengthens the resonance (see below). Off-resonance I_{PC} varied from ~ -1 to ~ -4 nA, but ΔI_{PC} was, of course, invariably 0. However, on resonance the transient ΔI_{PC} rises to +30 nA at $t = 39$ μs, i.e., $\Delta I_{PC}/I_{PC} \approx -30$. This is a colossal value for any magnetic resonance. The resonance is transient in that at sufficiently long times after switching the microwaves on (off), I_{PC} decays back to its off-resonance value. Thus, there is no dc ΔI_{PC}. However, in effect, it demonstrates a room-temperature magnetic resonance-induced switch if operated under alternating microwave power.

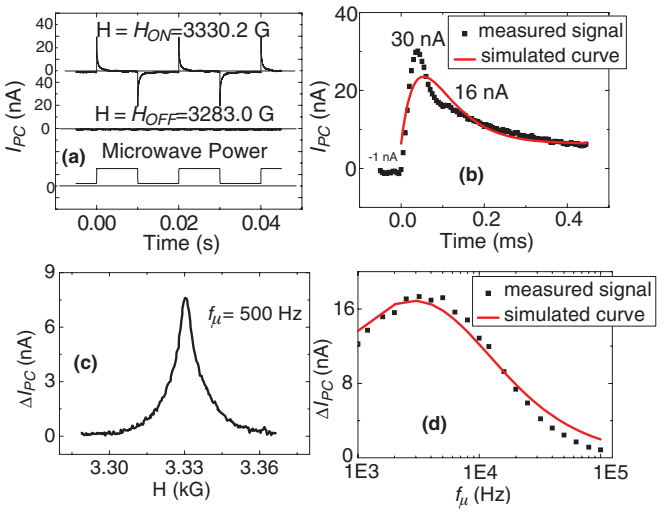

FIG. 1. (Color online) Colossal spin-1/2 PCDMR in MEH-PPV single-layer devices. (a) I_{PC} vs time t at $0 \leqslant t \leqslant 50$ ms at $H_{ON} =$ 3,330.2 G (upper trace) and $H_{OFF} = 3{,}283.0$ G (middle trace). The lower trace is the microwave power. (b) I_{PC} at H_{ON} vs t at $0 \leqslant t \leqslant 400\ \mu$s. The microwaves are turned on at $t = 0$. (c) ΔI_{PC} vs magnetic field using a lock-in amplifier. The microwave chopping frequency $f_\mu = 500$ Hz. (d) f_μ dependence of ΔI_{PC}.

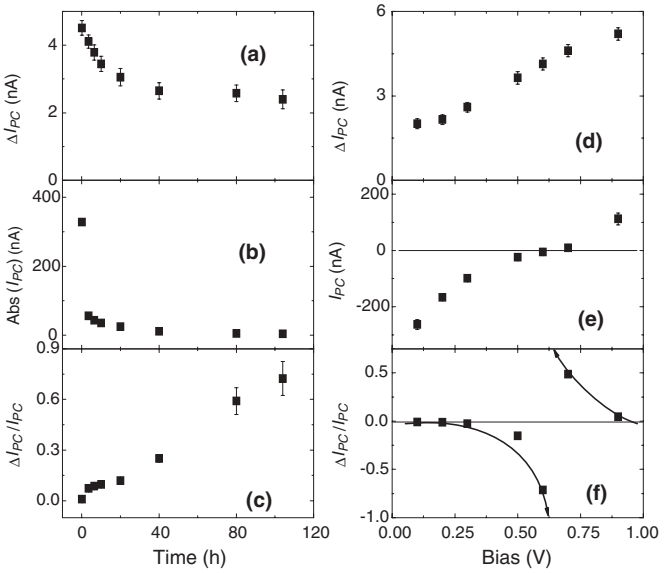

FIG. 2. The independence of ΔI_{PC} with respect to I_{PC}. (a)–(c) ΔI_{PC}, I_{PC}, and $\Delta I_{PC}/I_{PC}$ vs time, respectively, when the sample degraded in air. (d)–(f) ΔI_{PC}, I_{PC}, and $\Delta I_{PC}/I_{PC}$, respectively, vs bias. The lines are a guide to the eye.

To reduce noise, lock-in detection at f_μ was used in the cw comparisons. A typical room-temperature cw ΔI_{PC} is shown in Fig. 1(c). Note that the lock-in amplifier output gives only the time-averaged ΔI_{PC}. Thus, as Fig. 1(d) shows, this reading is f_μ dependent; unless otherwise specified, $f_\mu = 500$ Hz.

The PCDMR g value, 2.0027 ± 0.0003, is similar to that of the positive spin-1/2 p^+ polarons in MEH-PPV:[6,6]-phenyl C_{61}-butyric acid methyl ester (PCBM) and in poly(2-methoxy-5-(3-,7-dimethyloctyloxy)-1,4-phenylenevinylene) (MDMO-PPV):PCBM;[12,16] the p^+ are obviously on the PPV chains. The latter study resolved the g-tensor obtaining $g_{||} = 2.0034(1)$ and $g_\perp = 2.0024(1)$. The g values for p^+ are also consistent with a previous EDMR study on MEH-PPV devices,[17] where $2.001 \leqslant g \leqslant 2.003$. In contrast, for the negative spin-1/2 p^- polarons (electrons) on PCBM $g_x = 2.0003(1)$, $g_y = 2.0001(1)$, and $g_z = 1.9982(1)$.[16]

The foregoing EDMRs were all assigned to the strongly spin-dependent process:[3,5–7,12,17]

$$p^+ + p^+ \rightarrow bp^{++} + \text{phonons}. \qquad (1)$$

A synopsis of studies providing strong evidence for bipolarons in π-conjugated systems is given in the Appendix. The full width at half maximum we observed is ~18 G at a lowered microwave power $P_\mu = 40$ mW, which is also similar to the reported ~20-G-wide EDMR.[17]

Degradation increases $|\Delta I_{PC}/I_{PC}|$, mainly due to the decreased $|I_{PC}|$ [Figs. 2(a) and 2(b)]. Indeed, in another typical sample, $|I_{PC}|$ degraded by ~99% in 104 hr, from 328 to 4 nA, but ΔI_{PC} only degraded by ~44%, from 4.5 to 2.5 nA, and it stabilized at 2.5 nA after ~40 hr. This increased the cw $|\Delta I_{PC}/I_{PC}|$ with time [Fig. 2(c)]. After ~104 hr, it reached a value of 0.73, extremely strong for any magnetic resonance amplitude (the strongest resonance reported to date is $|\Delta I_{PC}/I_{PC}| \approx 0.03$ at 77 K),[4] and it continues to increase, albeit much more slowly.

The independence of ΔI_{PC} from I_{PC} can be further shown in biased PCDMR measurements on, e.g., relatively nondegraded samples [Figs. 2(d)–2(f)], where the Al was grounded and a positive V applied to the anode. As V increases to 0.9 V, ΔI_{PC} increases from 2.0 to 5.2 nA, while I_{PC} increases from −263 to +112 nA. $\Delta I_{PC}/I_{PC}$, of course, diverges when $I_{PC} \rightarrow 0$ at the open circuit voltage V_{OC}.

Although the PCDMR might be due to enhanced quenching of I_{PC} by enhanced bipolaron formation [Eq. (1)],[3,5–7,12,17] the degradation effect and especially the bias dependence cannot be explained by this mechanism. Any I_{PC}-quenching mechanism would limit ΔI_{PC} to $|I_{PC}|$. In particular, ΔI_{PC} would vanish when $I_{PC} \rightarrow 0$, in stark contrast to the observation.

The dark EDMR provides additional evidence that the PCDMR observed here originates from a different mechanism: Within the same bias range, no dark EDMR was observed, in contrast to EDMR and PCDMR of earlier PPV-based polymer light-emitting diodes.[3,7] This is not surprising as that EDMR amplitude $|\Delta I_{PC}/I_{PC}| < 10^{-4}$ is much weaker than the PCDMR observed here and too weak to be observed using the present setup.

Figure 3(a) compares Device A1, where the ITO/MEH-PPV was transferred into a vacuum chamber (pressure $\sim 10^{-6}$ torr) and pumped for 14 hr, to Device A2, where it was baked at 100 °C for 14 hr in flowing high-purity oxygen. The Al electrode was then thermally evaporated on both devices simultaneously. As seen, ΔI_{PC} is much stronger in Device A2 than in A1.

To understand the role of baking in O_2, several mechanisms were examined. First, exposure of the MEH-PPV film to O_2 for 14 hr at 100 °C should result in a higher concentration of oxidized Al at the MEH-PPV/Al interface, in effect creating an AlO_x buffer layer.[5,18,19] To examine whether this AlO_x is

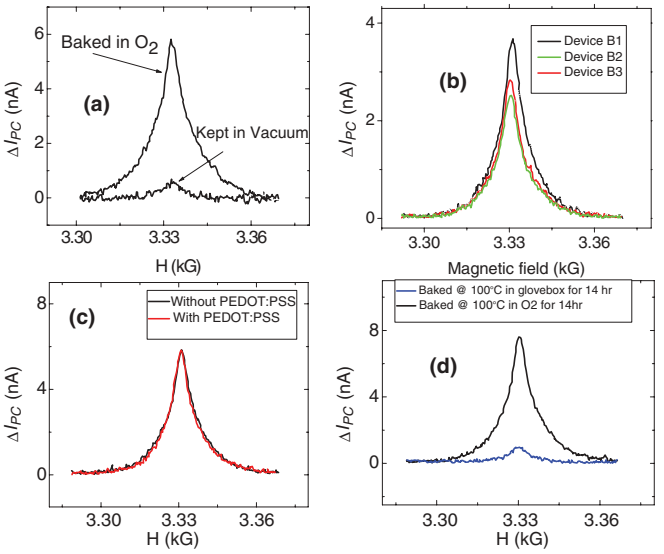

FIG. 3. (Color online) The effects on ΔI_{PC} of different fabrication treatments and structures (a) ΔI_{PC} vs H in devices with unoxidized and oxidized MEH-PPV films. (b) ΔI_{PC} vs H for Devices B1–B3, where the MEH-PPV layer was baked in O_2. Device B1: ITO/MEH-PPV/LiF (1 nm)/Al; Device B2: ITO/MEH-PPV/Al; Devices B3: ITO/MoO_3 (5 nm)/MEH-PPV/Al. (c) ΔI_{PC} vs H in Device C1 (ITO/PEDOT:PSS/MEH- PPV/Al) and Device C2 (ITO/MEH-PPV/Al), where the MEH-PPV layer was baked in O_2. (d) ΔI_{PC} vs H in devices baked at 100 °C for 14 hr in an Ar-filled glove box and in dry oxygen.

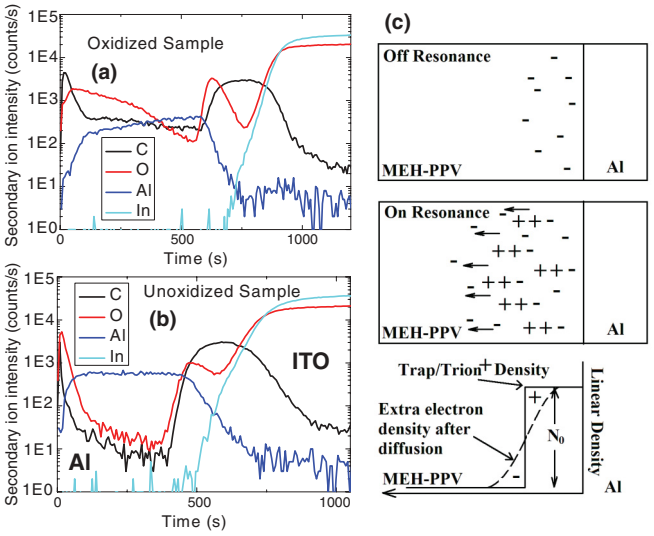

FIG. 4. (Color online) Possible mechanism for the spin-1/2 PCDMR (a) and (b) SIMS depth profiles of ITO/MEH-PPV/Al devices with the MEH-PPV layer (a) baked in oxygen and (b) left in vacuum overnight before Al deposition. (c) Suggested PCDMR mechanism: off resonance, traps near the Al/MEH-PPV interface are negative oxygen-related sites. Under resonance, these sites become positively charged by trion formation, which also releases extra electrons. While trions are pinned at these sites, the released electrons' diffusion creates an image current in the circuit.

responsible for the behavior of ΔI_{PC}, the following devices (all with MEH-PPV film baked in O_2) were compared (Fig. 3): ITO/MEH-PPV/1 nm LiF/Al (B1), ITO/5 nm MoO_x/MEH-PPV/Al (B2), and the reference ITO/MEH-PPV/Al (B3). $|I_{PC}|$ was much higher in Devices B1 and B2 than in B3; all values were measured before degradation. When excited at P_L = 10 mW/mm^2, Devices B1–B3 yielded $|I_{PC}| \sim 1.7$, 3.0, and 0.4 μA, respectively, indicating obvious differences in carrier transport. Yet ΔI_{PC} exhibited no such strong differences. Thus, the effect of oxygen baking on ΔI_{PC} is unlikely to be the result of improved carrier transport.

Another effect of baking MEH-PPV in O_2 could be the diffusion of oxygen and indium from ITO into MEH-PPV.[20–22] However, inserting a layer of poly(3,4-ethylenedioxythiophene): polystyrenesulfonate (PEDOT:PSS) between ITO and the polymer blocks such diffusion.[21] Hence, devices with a PEDOT:PSS layer between ITO and MEH-PPV (C1) were compared to devices without this layer (C2). As Fig. 3(c) shows, the devices yield similar ΔI_{PC}. Thus, the order-of-magnitude difference in ΔI_{PC} seen in Fig. 3(a) is not due to ITO dissociation. Additionally, Fig. 3(d) compares the devices with the MEH-PPV baked at 100 °C for 14 hr in an Ar-filled glove box (O_2 level < 5 ppm; D1) vs baked in dry oxygen (D2). As seen, ΔI_{PC} of Device D2 is much stronger than that of D1, again demonstrating that ΔI_{PC} is not due to oxygen or indium diffusion from ITO.

With the elimination of the foregoing mechanisms, we consider the formation of deep (0.75–0.91 eV) traps near the films' surface induced by exposure to air, as found by thermally stimulated luminescence studies on MEH-PPV films.[23] SIMS depth profiles of devices prepared as those compared in Fig. 3(a) are shown in Fig. 4. As seen, in the oxidized sample there is a rise in the oxygen concentration near the MEH-PPV/Al interface. In the MEH-PPV bulk (the region with the strongly increased carbon level), the oxygen level first decreases and then rises; the latter is probably due to the ITO, since it closely follows the In and Sn profiles. The peak oxygen level near the MEH-PPV/Al interface is consistent with our previous assumption: there are more oxygen-related deep traps near the interface and less in the bulk. In the nonoxidized MEH-PPV device, this peak is indeed much weaker. This is also consistent with our observation that ΔI_{PC} is greatly reduced if the sample is not intentionally oxidized [Fig. 3(a)]. Hence, this oxygen surplus originates from oxygen trapped in MEH-PPV during its oxidation.

It has been reported that bipolarons are stabilized by countercharges to form trions in PPVs.[6] We therefore assume that the oxygen-induced electron traps near the MEH-PPV/Al interface stabilize the $bp^{++}s$ to form positively charged trions. Magnetic resonance conditions would increase the trion density, as triplet (p^+, p^+) pairs would convert to singlet pairs and form spinless $bp^{++}s$. Naturally, the concentration profile of these trions would follow the deep oxygen-induced trap profile. Meanwhile, since the p^+s that contribute to the PCDMR are generated by exciton dissociation, the enhanced formation of trions releases more p^-s. Due to the concentration gradient near the interface, these electrons diffuse to the bulk, forming a dipole layer with the positive trions. The resonance-induced transient charge redistribution generates a transient image current observed as ΔI_{PC}, which is opposite to I_{PC}.

Figure 4(c) illustrates the model. When the microwaves are turned on, there is little ΔI_{PC} because the formation of

trions and electron release is not immediate; ΔI_{PC} peaks when the population of released electrons peaks. However, each electron will be eventually trapped. Hence, when the device approaches the new steady state at the resonance conditions, no net additional electrons are released, i.e., positive charges originating from bipolaron dissociation counterbalance newly released electrons. Note that the resonance-induced enhanced trion formation can also be viewed as resonance-induced enhanced hole trapping, which leads to a capacitance change, as observed in capacitance-detected magnetic resonance in inorganic devices.[24–26] However, the details of the trapping mechanisms are different in the two situations. Also, the relative capacitance change $\Delta C/C$ is only $\sim 10^{-7}$ in those inorganic devices vs ~ 1 in the cw PCDMR observed here.

Since ΔI_{PC} is largely determined by the oxygen concentration gradient, it degrades differently from I_{PC}. I_{PC} degradation can be caused by MEH-PPV photooxidation,[27] trap formation during operation,[28] etc. However, the trap-density gradient $\partial n(x,t)/\partial x$ evolution can be very different from the trap-density $n(x,t)$ evolution. For example, $\partial n(x,t)/\partial x$ can decrease, while $n(x,t)$ increases. In addition, the direction of the built-in field would not affect the sign of ΔI_{PC}. Adding a forward bias would, therefore, further separate the electrons from the trions and lead to a higher ΔI_{PC}, as observed in Fig. 2.

IV. THE TRAP GRADIENT MODEL

We now describe a quantitative model based on the scenario described above. For simplicity, we assume that the oxygen-induced trap concentration is a step function [see Fig. 4(c)]: near the MEH-PPV/Al interface, the concentration is high, and at some point toward the bulk, defined as $x = 0$, it drops to a negligible value throughout the bulk region.

Consider the global charge dipole $P(t)$ generated by the magnetic resonance-induced diffusion and trapping of extra electrons. This dipole can be visualized as composed of a fixed layer of positive trions near the Al cathode and the "free" electrons diffusing into the bulk of the MEH-PPV layer. In this scenario,

$$\Delta I_{PC} \propto dP(t)/dt. \tag{2}$$

Since the extra electrons diffuse throughout the MEH-PPV layer,

$$P(t) = \int_0^\infty qxn(x,t)dx, \tag{3}$$

where $q = 1.6 \times 10^{-19}$ C and $n(x,t)$ is the linear density of electrons at position x at time t; it is the sum of the linear densities of electrons generated between time t_G and $t_G + dt_G$:

$$n(x,t) = \int_0^t n'(x,t,t_G)dt_G. \tag{4}$$

Here, the upper bound for t_G is t because the generation must have occurred before the detection time t. Yet $n'(x, t, t_G)$ is governed by two processes: (i) electron generation at t_G followed by (ii) (re)distribution until t, including trapping at some time before t. Hence,

$$n'(x,t,t_G) = G(t_G)R(x,t,t_G), \tag{5}$$

where $G(t_G)$ is the generation rate of extra electrons at t_G and $R(x, t, t_G)$ is their normalized distribution function. We consider two possible contributions to R: (i) the contribution R_1 from electrons that diffuse freely until t; (ii) the contribution R_2 from electrons that become trapped before t (but after t_G). Within this scenario, R_1 is given by

$$R_1(x,t,t_G) = r_f(t')\frac{1}{2}\left[1 - \mathrm{erf}\left(\frac{x}{\sqrt{4D_{\mathrm{diff}}t'}}\right)\right], \tag{6}$$

where $r_f(t')$ is the fraction of these freely diffusing electrons, D_{diff} is their diffusion constant, and t' is the diffusion time.[29] Clearly, $t' = t - t_G$. For the contribution (ii) from trapped electrons, if the time that the electrons diffused before being trapped is s, we have

$$R_2(t') = \int_0^{t'} r_{tr}(s)\frac{1}{2}\left[1 - \mathrm{erf}\left(\frac{x}{\sqrt{4D_{\mathrm{diff}}s}}\right)\right]ds, \tag{7}$$

where $r_{tr}(s)$ is the fraction of electrons that become trapped between s and $s + ds$.

We can obtain expressions for $G(t_G)$, $r_f(t')$, and $r_{tr}(s)$ by considering the rate equations for trion generation and trapping of diffusing electrons. The generation of one trion releases two electrons:

$$G(t_G) = 2\frac{dn_{\mathrm{trion}}(t_G)}{dt_G}, \tag{8}$$

where $n_{\mathrm{trion}}(t_G)$ is the number of trions at t_G. We approximate the trion formation rate as

$$\frac{dn_{\mathrm{trion}}(t_G)}{dt_G} = -\frac{dN_{O_x^-}(t_G)}{dt_G} = \frac{N_{O_x^-}(t_G)}{\tau_1}, \tag{9}$$

where $N_{O_x^-}(t_G)$ is the number of negatively charged traps that are still available for trion formation at t_G and τ_1 is the (effective) characteristic time of trion formation at those sites. The solution for $N_{O_x^-}(t_G)$ is

$$N_{O_x^-}(t_G) = N_0 e^{-t_G/\tau_1}, \tag{10}$$

where N_0 is the number of traps at $t_G = 0$. In this model, it is proportional to the step height at $x = 0$. Thus, combining Eqs. (8)–(10), we have

$$G(t_G) = \frac{2N_0}{\tau_1}e^{-t_G/\tau_1}. \tag{11}$$

Now consider the trapping of electrons. Assuming the probability of trapping is the same for every electron, the number of diffusing electrons n_{diff} is given by

$$\frac{dn_{\mathrm{diff}}(s)}{ds} = -\frac{n_{\mathrm{diff}}(s)}{\tau_2}, \tag{12}$$

where τ_2 is the lifetime of these diffusing electrons. Therefore, the fraction of these freely diffusing electrons at $s = t'$ is

$$r_f(t') = e^{-t'/\tau_2}. \tag{13}$$

The fraction $r_{tr}(s)$ of electrons that become trapped between s and $s + ds$ is

$$r_{tr}(s) = \frac{1}{\tau}e^{-s/\tau_2}. \tag{14}$$

Substituting Eq. (13) into Eq. (6) and Eq. (14) into Eq. (7), then those new equations, together with Eq. (11) into Eq. (5), we

have an expression for $n'(x,t,t_G)$ that is inserted into Eq. (4). Then, we insert that expression for $n(x,t)$ into Eq. (3) to obtain the following expression for $P(t)$:

$$P(t)=\int_0^\infty qx\int_0^t \frac{N_0}{\tau_1}e^{-(t-t')/\tau_1}\left\{e^{-t'/\tau_2}\left[1-\mathrm{erf}\left(\frac{x}{\sqrt{4D_{\mathrm{diff}}t'}}\right)\right]+\int_0^{t'}\frac{e^{-s/\tau_2}}{\tau_2}\left[1-\mathrm{erf}\left(\frac{x}{\sqrt{4D_{\mathrm{diff}}s}}\right)\right]ds\right\}dt'dx$$
$$=\frac{\tau_2}{\tau_1}N_0qD_{\mathrm{diff}}\left(\tau_1+\frac{\tau_1^2}{\tau_2-\tau_1}e^{-t/\tau_1}-\frac{\tau_1\tau_2}{\tau_2-\tau_1}e^{-t/\tau_2}\right). \quad (15)$$

Thus,

$$\Delta I_{\mathrm{PC}}(t)\propto\frac{dP(t)}{dt}=\frac{N_0qD_{\mathrm{diff}}}{\tau_2-\tau_1}(e^{-t/\tau_2}-e^{-t/\tau_1}). \quad (16)$$

Obviously, this is a highly simplified analysis. For example, in modeling the diffusion of electrons, charge drift due to the built-in field and the Coulomb attraction between electrons and positively charged trions are neglected as they should, in first approximation, simply decrease the value of D_{diff}. Indeed, Figs. 1(b) and 1(d) demonstrate that, with $\tau_1 = 56$ μs and τ_2 842 μs, this simple model is in good agreement with the experimental results.

Importantly, as seen in Fig. 1(a), turning off the microwaves induces a transient PC that is essentially antisymmetric to the PCDMR observed when turning on the microwaves. In fact, the process following switching off can also be explained by our model. Once the resonance is turned off, with a lower probability of trion formation and thus lower equilibrium trion population, there is a net dissociation of positive trions in the trap-rich region and hence a net release of holes. This process mirrors the process of releasing electrons during trion formation in the switching-on situation. Thus, the calculations for microwave switching on (off) are valid for trion formation (dissociation) at a rate of $1/\tau_1$ followed by trapping of released electrons (holes) at a rate of $1/\tau_2$. A quantitative analysis is provided as follows:

Reconsidering the rate equation for trions in a more direct way, we have

$$\frac{dn_{\mathrm{trion}}}{dt}=-\frac{n_{\mathrm{trion}}}{\tau_{\mathrm{trion}}}+\gamma(N_0-n_{\mathrm{trion}}). \quad (17)$$

The first term on the right-hand side of the equation represents the dissociation of trions and the second term represents the formation of trions on available trap sites; γ represents the formation rate.

By rearranging the above equation,

$$\frac{dn_{\mathrm{trion}}}{dt}=-\left(\frac{1}{\tau_{\mathrm{trion}}}+\gamma\right)n_{\mathrm{trion}}+\gamma N_0. \quad (18)$$

Defining the *effective* trion formation rate as $1/\tau_1$,

$$\frac{1}{\tau_1}=\frac{1}{\tau_{\mathrm{trion}}}+\gamma, \quad (19)$$

the solution for the rate equation gives

$$\frac{dn_{\mathrm{trion}}}{dt}\propto\frac{1}{\tau_1}e^{-\frac{t}{\tau_1}}. \quad (20)$$

Comparing Eq. (20) with Eq. (10), τ_1 defined in Eq. (19) is the effective formation rate of trions defined in Eq. (10). Resonance conditions cause a small change in γ. Thus, turning the resonance on or off results in a small change only in $1/\tau_1$. Note that $\frac{dn_{\mathrm{trion}}}{dt}$ is proportional to the rate of released electrons under turn-on conditions and to the rate of released holes under turn-off conditions. Hence, the observed similarity in the transient signal when turning the microwaves on or off is not a coincidence and is explained well by our model.

The $\tau_2 \approx 0.84$ ms value is plausible given the low electron mobility $\mu_e \sim 10^{-7}$ cm^2/Vs in MEH-PPV;[30] using the Einstein relation, $D_{\mathrm{diff}} = \mu kT/q$ and $L = (D_{\mathrm{diff}}\tau)^{1/2}$ yields $D_{\mathrm{diff}} \sim 2.5 \times 10^{-9}$ cm^2 s^{-1} and a diffusion length $L \sim 15$ nm. Note that L of the electrons in the present scenario is likely <15 nm, as it is affected by the built-in field and the Coulomb attraction to the trions.

V. ON THE NATURE OF THE NEGATIVE OXYGEN CENTERS

The nature of the oxygen-induced traps is not clear. In one possible (irreversible) scenario PPV photo-oxidation cleaves the vinylene bond, and oxygen atoms attach to both carbons of the cleaved bond, forming aldehydes.[31,32] This apparently results from Dexter energy transfer from a PPV triplet exciton to the O_2 triplet ground state, resulting in the reactive singlet O_2, which cleaves the vinylene bond. In another plausible (at least partially reversible) scenario consistent with reported reversible processes,[32] photoinduced electron transfer from MEH-PPV to O_2 forms a MEH-PPV$^+$/O_2^- complex.[33]

In an attempt to assess the role of the two aforementioned scenarios, we compared the f_μ dependence of two samples from the same batch: In one the MEH-PPV film was baked for 14 hr at 100 °C in O_2 and then for 14 hr at 100 °C in an Ar-filled glove box prior to deposition of the Al. In the other the film was baked in the reverse order. The results, shown in Fig. 5, demonstrate that the difference is due to reversible O_2-induced processes, as O_2 is removed from the first sample during the 14-hr bake in the glove box. However, a contribution to the PCDMR by the irreversible process (known to occur

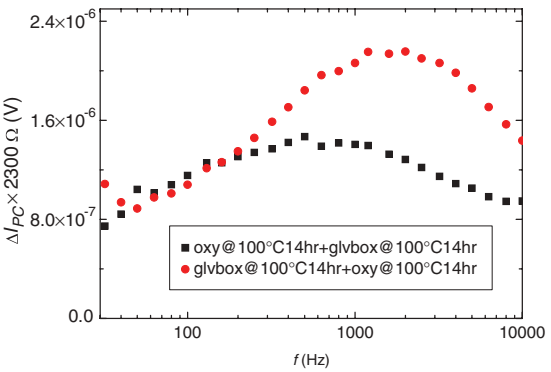

FIG. 5. (Color online) The microwave chopping frequency f_μ dependence of two samples from the same batch: In one (Sample I; solid black squares) the MEH-PPV film was baked for 14 hr at 100 °C in O_2 and then for 14 hr at 100 °C in an Ar-filled glove box before deposition of the Al cathode. In the other (Sample II; solid red circles), the film baking steps were conducted in the reverse order.

and evident by the irreversible reduction in I_{PC}) cannot be excluded.

VI. CONCLUSION

An extremely strong room-temperature PCDMR in ITO/MEH-PPV/Al devices, where the MEH-PPV film was baked overnight at 100 °C in O_2 is described, yielding, in effect, a magnetic resonance-induced switch. This change is largely independent of the off-resonance I_{PC}, rendering a huge cw $\Delta I_{PC}/I_{PC}$ when I_{PC} is small. The magnitude of this resonance is greatly strengthened by baking the MEH-PPV film in pure oxygen prior to Al deposition, indicating that the resonance is due to traps induced by oxygen exposure/baking. A plausible scenario involves enhanced formation of positive bipolarons stabilized by negatively charged oxygen-induced traps, i.e., trions. This results in dissociation of electron-hole pairs with released electrons diffusing toward the bulk, forming a dipole layer with the trions. The transient resonance-induced redistribution of electrons causes a transient "image current" in the circuit, which is observed as a very strong PCDMR. Simulations of this model are in good agreement with the experiments. The colossal resonance consequently identifies negative charge centers as potentially significant charge-trapping sites in organic devices, in particular solar cells.

ACKNOWLEDGMENTS

Ames Laboratory is operated by Iowa State University for the US Department of Energy (USDOE) under Contract No. DE-AC 02-07CH11358. This work was supported by the Office of Basic Energy Science, Division of Materials Sciences and Engineering, USDOE.

APPENDIX

Spinless bipolarons were invoked as excitations in π-conjugated polymers over 30 years ago. Direct EPR evidence for their presence was provided by Scott *et al.*;[34] additional early evidence was provided by Kaufman *et al.* and Colaneri *et al.*[35,36] Their properties were summarized in the classic review by Heeger *et al.*[37] Note, however, that the early theoretical studies of bipolarons generally ignored the Coulomb repulsion between the two like-charged polarons, focusing only on electron-lattice interactions believed to result in an attractive polaron-polaron interaction.

Bipolarons were invoked to explain ODMR and EDMR phenomena in π-conjugated polymers and organic light-emitting diodes (OLEDs) by Shinar, Friend, and coworkers who observed a *negative* spin-1/2 electroluminescence- (EL-) detected magnetic resonance (ELDMR) in the ELDMR studies of polymer LEDs.[3] Subsequently, they were also invoked to explain the *negative* spin-1/2 PLDMR observed in UV photoexcited π-conjugated materials.[38] In both cases it was assumed that their formation rate increases under magnetic resonance conditions (as they are spinless states generated by the spin-dependent coupling of two spin-1/2 polarons), and this increased formation rate increases the nonradiative quenching of singlet excitons by bipolarons, which reduces the EL and PL.

Additional strong evidence for the presence of bipolarons was given by combining the light-induced EPR (LEPR) work of De Ceuster *et al.* with the EDMR work of Silva *et al.*[16,17] The former unambiguously identified the g values and line shapes of the positive polarons in PPV derivatives and negative polarons in C_{60} derivatives. The EDMR observed by the latter was assigned to the spin-dependent fusion of two like-charged polarons to bipolarons. In agreement with these studies,[16,17] their results indicate that the narrower component is due to positive polarons, while the broader is due to negative polarons. As bipolarons are spinless and the resonance is due to spin-1/2 polarons with the narrower line shape, the mechanism is assigned to positive bipolaron generation by the coupling of two positive polarons.

A detailed treatment of the assumed role of bipolarons in both fluorescent and phosphorescent OLEDs was given by Li *et al.*[5,39] Notable recent studies invoking bipolarons include Kadashchuk *et al.*, Bobbert *et al.*, and Behrends *et al.*[6,8,12] In particular, Kadashchuk *et al.* concluded that due to the Coulomb repulsion between the two like-charged polarons, a counterpolaron is required to stabilize the bipolaron, creating, in effect, a trion.[6] Behrends *et al.* provided strong evidence for positive bipolaron formation and transport in MEH-PPV:PCBM photovoltaic devices by studying such devices containing an excess of PCBM under a forward bias of 1 V.[12]

*Corresponding authors: chenying@iastate.edu, jshinar@iastate.edu

[1] M.-K. Lee, M. Segal, Z. G. Soos, J. Shinar, and M. A. Baldo, Phys. Rev. Lett. **94**, 137403 (2005); M. Segal, M. A. Baldo, M. K. Lee, J. Shinar, and Z. G. Soos, Phys. Rev. B **71**, 245201 (2005).

[2] L. S. Swanson, J. Shinar, and K. Yoshino, Phys. Rev. Lett. **65**, 1140 (1990).

[3] L. S. Swanson, J. Shinar, A. R. Brown, D. D. C. Bradley, R. H. Friend, P. L. Burn, A. Kraft, and A. B. Holmes, Phys. Rev. B **46**, 15072 (1992); N. C. Greenham, J. Shinar, J. Partee, P. A. Lane, O. Amir, F. Lu, and R. H. Friend, *ibid.* **53**, 13528 (1996).

[4] V. Dyakonov, G. Rösler, M. Schwoerer, S. Blumstengel, and K. Lüders, J. Appl. Phys. **79**, 1556 (1996).

[5] G. Li, C. H. Kim, P. A. Lane, and J. Shinar, Phys. Rev. B **69**, 165311 (2004).

[6] A. Kadashchuk, V. I. Arkhipov, C. H. Kim, J. Shinar, D. W. Lee, Y. R. Hong, J. I. Jin, P. Heremans, and H. Bassler, Phys. Rev. B **76**, 235205 (2007).

[7] J. Shinar, Laser Photonics Rev. **6**, 767 (2012).

[8] P. A. Bobbert, T. D. Nguyen, F. W. A. van Oost, B. Koopmans, and M. Wohlgenannt, Phys. Rev. Lett. **99**, 216801 (2007).

[9] D. R. McCamey, H. A. Seipel, S. Y. Paik, M. J. Walter, N. J. Borys, J. M. Lupton, and C. Boehme, Nat. Mat. **7**, 723 (2008).

[10] D. R. McCamey, K. J. van Schooten, W. J. Baker, S. Y. Lee, S. Y. Paik, J. M. Lupton, and C. Boehme, Phys. Rev. Lett. **104**, 017601 (2010).

[11] T. D. Nguyen, G. Hukic-Markosian, F. Wang, L. Wojcik, X.-G. Li, E. Ehrenfreund, and Z. V. Vardeny, Nat. Mat. **9**, 345 (2010).

[12]J. Behrends, A. Schnegg, K. Lips, E. A. Thomsen, A. K. Pandey, I. D. W. Samuel, and D. J. Keeble, Phys. Rev. Lett. **105**, 176601 (2010).
[13]Z. H. Xiong, D. Wu, Z. V. Vardeny, and J. Shi, Nature (London) **427**, 821 (2004).
[14]S. Pramanik, C.-G. Stefanita, S. Patibandla, S. Bandyopadhyay, K. Garre, N. Harth, and M. Cahay, Nat. Nanotechnol. **2**, 216 (2007).
[15]W. J. M. Naber, S. Faez, and W. G. van der Wiel, J. Phys. D **40**, R205 (2007).
[16]J. De Ceuster, E. Goovaerts, A. Bouwen, J. C. Hummelen, and V. Dyakonov. Phys. Rev. B **64**, 195206 (2001).
[17]G. B. Silva, L. F. Santos, R. M. Faria, and C. F. O. Graeff, Physica B **308-310**, 1078 (2001).
[18]K. Demirkan, A. Mathew, C. Weiland, M. Reid, and R. L. Opila, J. Appl. Phys. **103**, 034505 (2008).
[19]F. Li, H. Tang, J. Anderegg, and J. Shinar, Appl. Phys. Lett. **70**, 1233 (1997).
[20]J. C. Scott, J. H. Kaufman, P. J. Brock, R. DiPietro, J. Salem, and J. A. Goitia, J. Appl. Phys. **79**, 2745 (1996).
[21]T. P. Nguyen, P. L. Rendu, N. N. Dinh, M. Fourmigue, and C. Mézière, Synth. Met. **138**, 229 (2003).
[22]M. P. de Jong, L. J. van IJzendoorn, and M. J. A. de Voigt, Appl. Phys. Lett. **77**, 2255 (2000).
[23]V. Kažukauskas, H. Tzeng, and S. A. Chen, Appl. Phys. Lett. **80**, 2017 (2002).
[24]M. Stutzmann, M. S. Brandt, and M. W. Bayel, Non-Cryst. Solids **1–22**, 266 (2000).
[25]M. S. Brandt, R. T. Neuberger, and M. Stutzmann, Appl. Phys. Lett. **76**, 1467 (2000).
[26]M. S. Brandt, R. T. Neuberger, M. W. Bayel, and M. Stutzmann, Jpn. J. Appl. Phys. **38**, 1172 (1999).
[27]D. G. J. Sutherland, J. A. Carlisle, P. Elliker, G. Fox, T. W. Hagler, I. Jimenez, H. W. Lee, K. Pakbaz, L. J. Terminello, S. C. Williams, F. J. Himpsel, D. K. Shuh, W. M. Tong, J. J. Jia, T. A. Callcott, and D. L. Ederer, Appl. Phys. Lett. **68**, 2046 (1996).
[28]G. C. M. Silvestre, M. T. Johnson, A. Giraldo, and J. M. Shannon, Appl. Phys. Lett. **78**, 1619 (2001).
[29]J. Crank, *The Mathematics of Diffusion* (Clarendon Press, Oxford, England, 1975), Chap. 2.
[30]L. Bozano, S. A. Carter, J. C. Scott, G. G. Malliaras, and P. J. Brock, Appl. Phys. Lett. **74**, 1132 (1999).
[31]M. Yan, L. J. Rothberg, F. Papadimitrakopoulos, M. E. Galvin, and T. M. Miller, Phys. Rev. Lett. **73**, 744 (1994).
[32]B. H. Cumpston, I. D. Parker, and K. F. Jensen, J. Appl. Phys. **81**, 3716 (1997).
[33]S.-J. Park, A. J. Gesquiere, J. Yu, and P. F. Barbara, J. Am. Chem. Soc. **126**, 4116 (2004).
[34]J. C. Scott, P. Pfluger, M. T. Krounbi, and G. B. Street, Phys. Rev. B **28**, 2140 (1983).
[35]J. H. Kaufman, N. Colaneri, J. C. Scott, and G. B. Street, Phys. Rev. Lett. **53**, 1005 (1984).
[36]N. Colaneri, M. Nowak, D. Spiegel, S. Hotta, and A. J. Heeger, Phys. Rev. B **36**, 7964 (1987).
[37]A. J. Heeger, S. Kivelson, J. R. Schrieffer, and W.-P. Su, Rev. Mod. Phys. **60**, 781 (1988).
[38]J. Shinar, A. V. Smith, P. A. Lane, K. Yoshino, Y. W. Ding, and T. J. Barton, Mol. Cryst. Liq. Cryst. **256**, 691 (1994).
[39]G. Li, J. Shinar, and G. E. Jabbour, Phys. Rev. B **71**, 235211 (2005).